17 Topological Methods for Flow Visualization

GERIK SCHEUERMANN and XAVIER TRICOCHE
University of Kaisersluatern, Germany

17.1 Introduction

Numerical simulations provide scientists and engineers with an increasing amount of vector and tensor data. The visualization of these large multivariate datasets is therefore a challenging task. Topological methods efficiently extract the structure of the corresponding fields to come up with an accurate and synthetic depiction of the underlying flow. This approach takes its roots and inspiration in the visionary work of Poincaré at the end of the 19th century. Practically, it consists of partitioning the domain of study into subregions of homogeneous qualitative behavior. Extracting and visualizing the corresponding graph permits conveyance of the most meaningful properties of multivariate datasets. This has motivated the design of various topology-based visualization schemes. This chapter proposes an introduction to the theoretical foundations of the topological approach and presents an overview of the corresponding visualization methods. Emphasis is put on recent advances. In particular, the processing of turbulent or unsteady vector and tensor fields is addressed.

Vector and tensor fields are traditionally objects of major interest for visualization. They are the mathematical language of many research and engineering areas, for example, fundamental physics, optics, solid mechanics, and fluid dynamics, as well as civil engineering, aeronautics, turbomachinery, or weather forecast. Vector variables in this context are velocity, vorticity, magnetic or electric field, and a force or the gradient of some scalar field like e.g., temperature. Tensor variables might correspond to stress, strain, or rate of deformation, for instance. From a theoretical viewpoint, vector and tensor fields have received much attention from mathematicians, leading to a precise and rigorous framework that constitutes the basis of specific visualization methods. Of particular interest is Poincaré's work [20], which laid down the foundations of a geometric interpretation of vector fields associated with dynamical systems at the end of the 19th century; the analysis of the phase portrait provides an efficient and aesthetic way to apprehend the information contained in abstract vector data. Nowadays, following this theoretical inheritance, scientists typically focus their study on the topology of vector and tensor datasets provided by Computational Fluid Dynamics (CFD) or Finite Element Methods. A typical and very active application field is fluid dynamics, in which complex structural behaviors are investigated in the light of their topology [14,27,19,3]. It was shown, for instance, that topological features are directly involved in crucial aspects of flight stability like flow separation or vortex genesis [4]. Informally, the topology is the qualitative structure of a multivariate field. It leads to a partition of the domain of interest into subdomains of equivalent qualitative nature. Therefore, extracting and studying this structure permits us to focus the analysis on essential properties. For visualization purposes, the depiction of the topology results in synthetic representations that transcribe the fundamental characteristics of the data. Moreover, it permits fast extraction of global flow structures that are directly related to features of interest in various practical applications. Further, topology-based visualization results in a dramatic decrease in the amount of data necessary for interpretation, which makes it very appealing for the analysis of large-scale datasets. These ideas are at the basis of the topological approach, which has gained an increasing interest in the visualization community during the last decade. First introduced for planar vector fields by Helman and Hesselink [9], the basic technique has been continuously extended since then. A significant milestone on the way was the work of Delmarcelle [5], which transposed the original vector method to symmetric, second-order tensor fields.

The contents of this survey are organized as follows. Vector fields are considered first. Basic theoretical notions are introduced in Section 17.2. They result from the qualitative theory of dynamical systems, initiated by Poincaré's work. Nonlinear and parameter-dependent topologies are discussed in this section, along with the fundamental concept of bifurcation. Tensor fields are treated in Section 17.3. Following Delmarcelle's approach, we are concerned with the topology of the eigenvector fields of symmetric, second-order tensor fields. It is shown that they induce line fields in which tangential curves can be computed, analogous to streamlines for vector fields. We explain how singularities are defined and characterized and how bifurcations affect them in the case of unsteady tensor fields. This completes the framework required for the description of topology-based visualization of vector and tensor fields in Section 17.4. The presentation covers original methods for 2D and 3D fields, extraction and visualization of nonlinear topology, topology simplification for the processing of turbulent flows, and topology tracking for parameter-dependent datasets. Finally, Section 17.5 completes the presentation by addressing open questions and suggesting future research directions to extend the scope of topology-based visualization.

17.2 Vector Field Topology

In this section, we propose a short overview of the theoretical framework of vector-field topology, which we restrict to the requirements of visualization techniques.

17.2.1 Basic Definitions

We consider a vector field $\boldsymbol{v} : U \subseteq \mathbb{R}^n \times \mathbb{R} \rightarrow T\mathbb{R}^n \simeq \mathbb{R}^n$, which is a vector-valued function that depends on a space variable and on an additional scalar parameter, say time. The vector field $\boldsymbol{v}$ generates a *flow* $\phi_t : U \subseteq \mathbb{R}^n \rightarrow \mathbb{R}^n$, where $\phi_t := \phi(x, t)$ is a smooth function defined for $(\boldsymbol{x}, t) \in U \times (I \subseteq \mathbb{R})$ satisfying

$$\frac{d}{dt}\phi(x, t)|_{t=\tau} = v(\tau, \phi(x, \tau)) \tag{17.1}$$

for all $(\boldsymbol{x}, \tau) \in U \times I$. Practically we limit our presentation to the case $n = 2$ or 3 in the following. The function $\phi(\boldsymbol{x}_0, :) : t \rightarrow \phi(x_0, t)$ is an *integral curve* through $\boldsymbol{x}_0$. Observe that existence and uniqueness of integral curves are ensured under the assumption of fairly general continuity properties of the vector field. In the special but fundamental case of steady vector fields, i.e., fields that do not depend on the variable t, integral curves are called *streamlines*. Otherwise, they are called *pathlines*. The uniqueness property guaranties that streamlines cannot intersect in general. The set of all integral curves is called *phase portrait*, according to Poincaré's original formulation. The qualitative structure of the phase portrait is called topology of the vector field. First we focus on the steady case, and then we consider parameter-dependent topology. Q1

17.2.2 Steady Vector Fields

The local geometry of the phase portrait is characterized by the nature and position of its *critical points*. In the steady case, these *singularities* are locations where the vector field is zero. Consequently, they behave as zero-dimensional integral curves. Furthermore, they are the only positions where streamlines can intersect (asymptotically). Basically, the qualitative study of critical points relies on the properties of the Jacobian matrix of the vector field at their position. If the Jacobian has full rank, the critical points is said to be linear or of *first order*. Otherwise, a critical point is of *higher order*. Next we discuss the planar and 3D cases successively. Observe that considerations made for 2D vector fields also apply to vector fields defined over a 2D manifold embedded in three dimensions, for example, the surface of an object surrounded by a 3D flow.

17.2.2.1 Planar case

Planar critical points have benefited from great attention from mathematicians. A complete classification has been provided by Andronov et al. [1]. Additional excellent information is available in Abraham and Shaw [2] and Hirsch and Smale [12]. Depending on the real and imaginary parts of the eigenvalues, linear critical points may exhibit the configurations shown in Fig. 17.1. Repelling singularities act as *sources*, whereas attracting ones are *sinks*. *Hyperbolic* critical points are a subclass of linear singularities for which both eigenvalues have nonzero real parts. Thus, a center is nonhyperbolic. The analysis of nonlinear critical points, on the contrary, requires us to take into account higher-order polynomial terms in the Taylor expansion. Their vicinity is decomposed into an arbitrary combination of *hyperbolic, parabolic*, and *elliptic* curvilinear sectors, see Fig. 17.2. The bounding curve of a hyperbolic sector is called a *separatrix*. Back in the linear case, separatrices only exist for saddle points, where they are the four curves

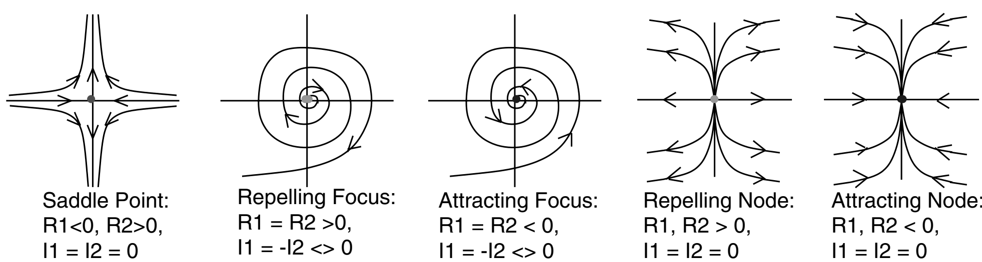

Figure 17.1 Basic configurations of first-order planar critical points

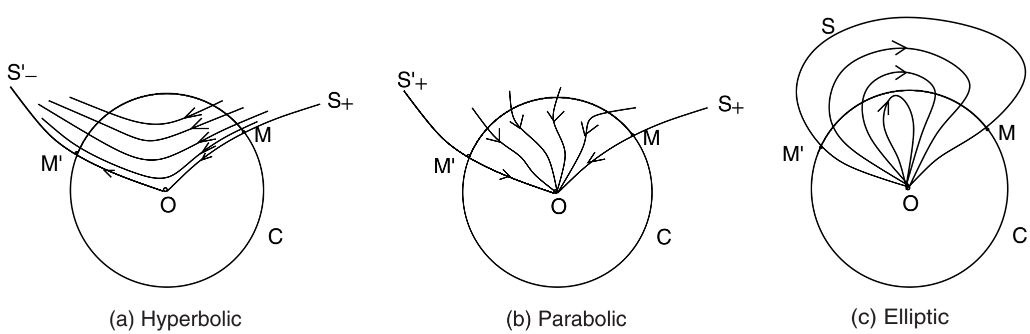

Figure 17.2 Sector types of arbitrary planar critical points

that reach the singularity, forward or backward in time. Thus, we obtain a simple definition of planar topology as the graph whose vertices are the critical points and whose edges are the separatrices integrated away from the corresponding singularities. This needs to be completed by *closed orbits* that are periodic integral curves. Closed orbits play the role of sources or sinks and can be seen as additional separatrices. It follows that topology decomposes a vector field into subregions where all integral curves have a similar asymptotic behavior: they converge toward the same critical point (resp. closed orbit) both forward and backward. We complete our overview of steady planar topology by mentioning the *index* of a critical point introduced by Poincaré in the qualitative theory of dynamic systems. It measures the number of field rotations along a closed curve that is chosen to be arbitrarily small around the critical point. By continuity of the vector field, this is always a (signed) integer value. The index is an invariant quantity for the vector field and possesses several properties that explain its importance in practice. Among them we have the following:

1. The index of a curve that encloses no critical point is zero,
2. The index of a linear critical point is -1 for a saddle point and $+1$ for every other type (Fig. 17.3),
3. The index of a closed orbit is always $+1$,
4. The index of a curve enclosing several critical points is the sum of their individual indices.

17.2.2.2 Three-dimensional case

The 3D case lacks an analogous intensive theoretical treatment. To our knowledge, there exists no exhaustive characterization of arbitrary 3D critical points, i.e., there is no generalization to 3D of the sector-type decomposition achieved by Andronov. Therefore, we address only linear 3D critical points. Like the planar case, the analysis is based on the eigenvalues of the Jacobian. There are two main possibilities: either the eigenvalues are all real or two of them are complex conjugates.

- *Three real eigenvalues*. One has to distinguish the case where all three eigenvalues have the same sign, where we have a 3D node (either attracting or repelling) from the case where only two eigenvalues have the same sign: the two eigenvectors associated with the eigenvalues of the same sign span a plane in which the vector field behaves as a 2D node and the critical point is a 3D saddle.
- *Two complex eigenvalues*. Once again there are two possibilities. If the common real part of both complex eigenvalues has the same sign as the real eigen-value, one has a 3D spiral, i.e., a critical point (either attracting or repelling) that exhibits a 2D spiral structure in the plane spanned by the eigenspace related to the complex eigenvalues. If they have different signs, one has a second kind of 3D saddle.

Refer to Fig. 17.4 for a visual impression. Analoguous to the planar case, a critical point is called *hyperbolic* in this context if the eigen-

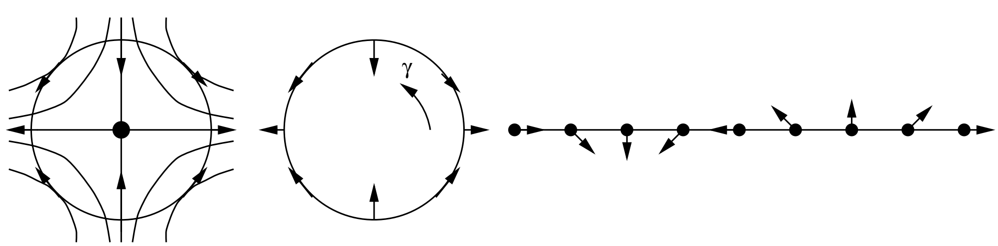

Figure 17.3 Simple closed curve of index -1 (saddle point)

values of the Jacobian have all nonzero real parts. Compared to 2D critical points, separatrices in 3D are not restricted to curves; they can be surfaces, too. These surfaces are called streamsurfaces and are constituted by the set of all streamlines that are integrated from a curve. The linear 3D topology is thus composed of nodes, spirals, and saddles that are interconnected by curve and surface separatices emanating from saddle points. These are, in fact the eigenspaces corresponding to the eigenvalues with positive, resp. negative real part, started in the vicinity of the critical point and integrated away. Depending on the considered type, repelling and attracting eigenspaces can be ID or 2D, leading to curves and surfaces (Figs. 17.4b and 17.4d).

Q2

17.2.3 Parameter-Dependent Vector Fields

The previous sections focused on steady vector fields. Now, if the considered vector field depends on an additional parameter, the structure of the phase portrait may transform as the value of this parameter evolves: position and nature of critical points can change along with the connectivity of the topological graph. These modifications—called *bifurcations* in the literature—are continuous evolutions that bring the topology from a stable state to another, structurally consistent, stable state. Bifurcations have been the subject of an intensive research effort in pure and applied mathematics [7]. The present section will provide a short introduction to these notions. Notice that the treatment of 3D bifurcations is beyond the scope of this paper, since they have not been applied to flow visualization up till now. We start with basic considerations about structural stability and then describe typical planar bifurcations.

17.2.3.1 Structural stability

As said previously, bifurcations consist of topological transitions between stable structures. In fact, the definition of structural stability involves the notion of structural equivalence. Two vector fields are said to be *equivalent* if there exists a diffeomorphism (i.e., a smooth map with smooth inverse) that takes the integral curves of one vector field to those of the second while preserving orientation. *Structural stability* is now defined as follows: the topology of a vector field v is stable if any perturbation of v, chosen small enough, results in a vector field that is structurally equivalent to v. We can now state a simplified version of the fundamental Peixoto's theorem [7] on structural stability for 2D flows. *A smooth vector field on a two-dimensional compact planar domain of* $I\!R^2$ *is structurally stable if and only if (*iff*) the number of critical points and closed orbits is finite and each is hyperbolic, and if there are no integral curves connecting saddle points*. Practically, Peixoto's theorem implies that a planar vector field typically presents saddle points, sinks, and sources, as well as attracting or repelling closed orbits. Furthermore, it asserts that nonhyperbolic critical points or closed orbits are unstable because small perturbations Q3

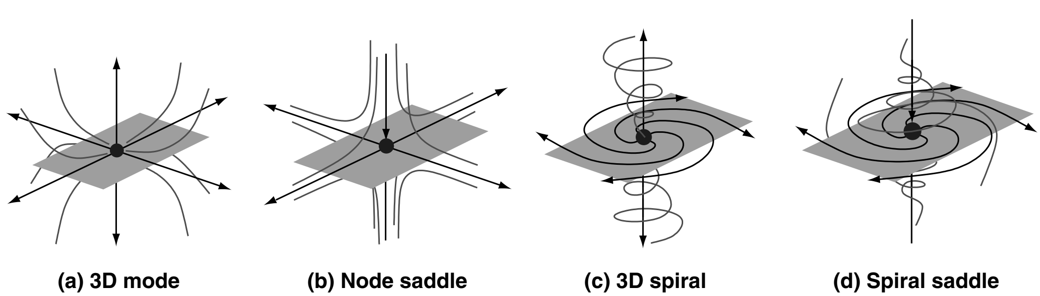

Figure 17.4 Linear 3D critical points

can make them hyperbolic. Saddle connections, as far as they are concerned, can be broken by small perturbations as well.

17.2.3.2 Bifurcations

There are two types of structural transitions: local and global bifurcations.

Local Bifurcations

There are two main types of local bifurcations affecting the nature of a singular point in 2D vector fields. The first one is the so-called *Hopf bifurcation*. It consists of the transition from a sink to a source with simultaneous emission of a surrounding closed orbit that behaves as a sink, preserving local consistency with respect to the original configuration (Fig. 17.5). At the bifurcation point there is a center. The reverse evolution is possible too, as is an inverted role of sinks and sources. A second typical local bifurcation is called *Fold Bifurcation* and consists of the pairwise annihilation or
Q4 creation of a saddle and a sink (resp. source). This evolution is depicted in Fig. 6. Observe that the index of the concerned region remains 0 throughout the transformation.

Global Bifurcations

In contrast to the cases mentioned above, global bifurcations do not take place in a small neighborhood of a singularity, but entail significant changes in the flow structure and involve large domains by modifying the connectivity of the topological graph. Actually, global bifurcations still remain a challenging topic for mathematicians. Consequently, we mention here just a typical configuration exhibited by such transitions: the unstable saddle–saddle connection (see Peixoto's theorem). This is the central constituent of *basin bifurcations*, where the relative positions of two separatrices emanating from two neighboring saddle points are swapped through a saddle–saddle separatrix.

17.3 Tensor-Field Topology

Making use of the results obtained for vector fields, we now turn to tensor-field topology. We adopt for our presentation an approach similar to the original work of Delmarcelle [5,6], and focus on symmetric second-order real tensor fields that we analyze through their eigenvector fields. We seek here a framework that permits us to extend the results discussed previously to tensor fields. However, since most of the research done so far has been concerned with the 2D case, we put the emphasis on planar tensor fields and point out the generalization to 3D fields. A mathematical treatment of these notions can be found in Tricoche [28], where it is shown how covering spaces allow association of a line field with a vector field. In this section, we first introduce useful notations in the steady case and also show how symmetric second-order tensor fields can be interpreted as line fields. This makes possible the integration of tangential curves called tensor lines. Next, singularities are considered. We complete the presentation with tensor bifurcations.

17.3.1 Line Fields

17.3.1.1 Basic definitions

In the following, we call a symmetric second-order real tensor of dimension 2 or 3. This is a Q5

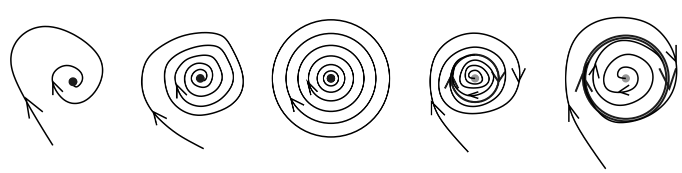

Figure 17.5 Hopf bifurcation

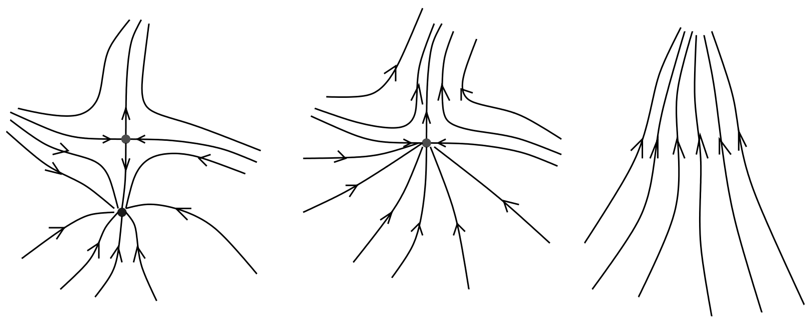

Figure 17.6 Pairwise annihilation

geometric invariant that corresponds to a linear transformation and can be represented by a matrix in a cartesian basis. By extension, we define a tensor field as a map T that associates every position of a subset of the euclidean space $I\!R^n$ with a $n \times n$ symmetric matrix. Thus, it is characterized by $\frac{1}{2}n(n+1)$ independent, real scalar functions. Note that an arbitrary second-order tensor field can always be decomposed into its symmetric and antisymmetric parts. From the structural point of view, a tensor field is fully characterized by its *deviator field*, which is obtained by subtracting from the tensor its isotropic part, that is $\mathrm{D} = \mathrm{T} - \frac{1}{n}(\mathrm{tr\ T})\mathrm{I}_n$, where tr T is the trace of T and I_n the identity matrix in $I\!R^n$. Observe that the deviator has trace zero by definition. The analysis of a tensor field is based on the properties of its eigensystem. Since we consider symmetric tensors, the eigenvectors always form an orthogonal basis of $I\!R^n$ and the eigenvalues are real. It is a well known fact that eigenvectors are defined modulo a nonzero scalar, which means that they have neither inherent norm nor orientation. This characteristic plays a fundamental role in the following process. Through its corresponding eigensystem, any symmetric real tensor field can now be associated with a set of orthogonal eigenvector fields. We choose the following notations in three dimensions. *Let* $\lambda_1 > \lambda_2 > \lambda_3$ *be the real eigenvalues of the symmetric tensor field* T (*i.e.*, λ_1, λ_2, and λ_3 *are scalar fields as functions of the coordinate vector* x*). The corresponding eigenvector fields* e_1, e_2, *and* e_3 *are respectively called* major, medium, *and* minor eigenvector fields. In the 2D case, there are just major and minor eigenvectors. We now come to tensor lines, which are the object of our structural analysis.

Q6

Q7

17.3.1.2 Tensor lines

A *tensor line* computed in a Lipschitz continuous eigenvector field is a curve that is everywhere tangent to the direction of the field. Because of the lack of both norm and orientation, the tangency is expressed at each position in the domain in terms of lines. For this reason, an eigenvector field corresponds to a *line field*. Nevertheless, except at positions where two (or three) eigenvalues are equal, integration can be carried out in a way similar to streamlines for vector fields by choosing an arbitrary local orientation. Practically, this consists of determining a continuous angular function θ^* defined modulo 2π that is everywhere equal to the angular coordinate θ of the line field, modulo π. Considering the set of all tensor lines as a whole, the topology of a tensor field is defined as the structure of the tensor lines. It is interesting to observe that the topologies of the different eigenvector fields can be deduced from another through the orthogonality of the corresponding line fields. Q8

17.3.2 Degenerate points

The inconsistency in the local determination of an orientation as described previously only occurs in the neighborhood of positions where several eigenvalues are equal. There, the eigenspaces associated with the corresponding eigenvalues are no longer 1D. For this reason, such positions are singularities of the line field. To remain consistent with the notations originally used by Delmarcelle, we call them *degenerate points*, though they are typically called *umbilic points* in differential geometry. Because of the direction indeterminacy at degenerate points, tensor lines can meet there, which underlines the analogy with critical points.

17.3.2.1 Planar case

The deviator part of a 2D tensor field is zero *iff* both eigenvalues are equal. For this reason, degenerate points correspond to zero values of the deviator field. Thus, D can be approximated as follows in the vicinity of the degenerate point P_0:

$$\mathrm{D}\,(P_0 + d\boldsymbol{x}) = \nabla\mathrm{D}\,(P_0)d\boldsymbol{x} + o(d\boldsymbol{x}) \tag{17.2}$$

Where $d\boldsymbol{x} = (x, y)^T$, and where α and β are real scalar functions on $I\!R^2$,

$$\mathrm{D}(x,y) = \begin{pmatrix} \alpha & \beta \\ \beta & -\alpha \end{pmatrix}, \text{ and } \nabla\mathrm{D}\,(P_0)d\boldsymbol{x} = \begin{pmatrix} \frac{\partial\alpha}{\partial x}dx + \frac{\partial\alpha}{\partial y}dy & \frac{\partial\beta}{\partial x}dx + \frac{\partial\beta}{\partial y}dy \\ \frac{\partial\beta}{\partial x}dx + \frac{\partial\beta}{\partial y}dy & -\frac{\partial\alpha}{\partial x}dx - \frac{\partial\alpha}{\partial y}dy \end{pmatrix}$$

If the condition $\frac{\partial\alpha}{\partial x}\frac{\partial\beta}{\partial y} - \frac{\partial\alpha}{\partial y}\frac{\partial\beta}{\partial x} \neq 0$ holds, the degenerate point is said to be linear. The local structure of the tensor lines in this vicinity depends on the position and number of radial directions. If θ is the local angle coordinate of a point with respect to the degenerate point, $u = tan\theta$ is the solution of the following cubic polynomial:

$$\beta_2 u^3 + (\beta_1 + 2\alpha_2)u^2 + (2\alpha_1 - \beta_2)u - \beta_1 = 0 \tag{17.3}$$

with $\alpha_1 = \frac{\partial\alpha}{\partial x}, \alpha_2 = \frac{\partial\alpha}{\partial y}$, and the same for β_i. This equation has either one or three real roots, which all correspond to angles along which the tensor lines asymptotically reach the singularity. These angles are defined modulo π, so one obtains up to six possible angle solutions. Since we limit our discussion to a single (minor/major) eigenvector field, we are finally concerned with up to three radial eigenvectors. The possible types of linear degenerate points are trisectors and wedges (Fig. 17.7). In fact, the special importance of radial tensor lines is explained by their interpretation as separatrices. As a matter of fact, like critical points, the set of all tensor lines in the vicinity of a degenerate point is partitioned into hyperbolic, parabolic, and elliptic sectors. Separatrices are again defined as the bounding curves of the hyperbolic sectors (compare Fig. 17.7). In fact, a complete definition of the planar topology involves *closed tensor lines* too. However, they are rare in practice. The analogy with vector fields may be extended by defining the tensor index of a de-

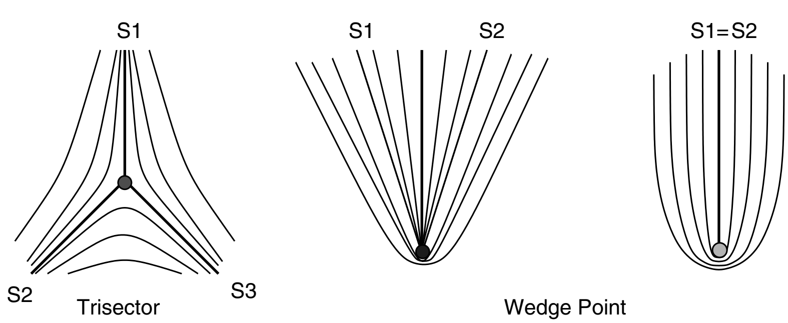

Figure 17.7 Linear degenerate points in the plane.

generate point [5,28] that measures the number of rotations of a particular eigenvector field along a closed curve surrounding a singularity. Notice that tensor indices are half integers, due to orientation indeterminacy: trisectors have index $-\frac{1}{2}$ and wedges have index $\frac{1}{2}$. The nice properties of Poincaré's index extend here in a very intuitive fashion.

17.3.2.2 Three-dimensional degenerate points

In the 3D case, singularities are of two types: eigenspaces may become 2D or 3D, leading to tangency indeterminacy in the corresponding eigenvector fields. To simplify the presentation, we restrict our considerations to the trace-free deviator $\mathrm{D} = (D_{ij})_{i,j}$. The characteristic equation is $-\lambda^3 + b\lambda + c = 0$, where $-c$ is the determinant of D and $b = \frac{1}{2}\sum_i D_{ii} + \sum_{i<j} D_{ij}^2$. The quantity $\Delta = (\frac{c}{2})^2 - (\frac{b}{3})^3$ determines the number of distinct real roots of the equation: $\Delta < 0$ yields three distinct real roots, while there are multiple roots *iff* $\Delta = 0$ (complex conjugate roots are impossible, since D is symmetric). Thus, degeneracies correspond to a maximum of Δ, which is everywhere negative, except at points, lines, or surfaces, where it is zero. Here a major difference with 3D vector-field topology must be underlined: The loci of singularities are not restricted to points. Refer to Hesselink et al. [11] and Lavin et al. [16] for additional information.

17.3.3 Parameter-Dependent Topology

Again, the natural question that arises at this stage is the structural stability of topology under small perturbations of an underlying parameter. We restrict our considerations to the simplest cases in 2D of local and global bifurcations to remain in the scope of the methods to come. The observations proposed next are all inspired by geometric considerations.

Following the basic idea behind Peixoto's theorem, we see that the only stable degenerate points must be the linear ones. As a matter of fact, the asymptotic behavior of tensor lines in the vicinity of a degenerate point is determined by the third-order differential ∇D (thus leading to a linear degenerate point) except at locations where it becomes singular. This is, by essence, an unstable property, since arbitrary small perturbations in the coefficients lead to one of the linear configurations. Continuing our analogy with the vector case, we conclude that integral curves are unstable if they are separatrices for both of the degeneracies they link together. This is because a small-angle perturbation of the line field around any point along the separatrix suffices to break the connection. Using these elementary results, we review typical planar bifurcations.

17.3.3.1 Pairwise creation and annihilation

Since a wedge and a trisector have opposite indices, a closed curve enclosing them has index 0. This simple fact is the basic idea behind pairwise creations or annihilations. Indeed, the zero index computed along this closed curve shows that the combination of both degenerate points is structurally equivalent to a uniform flow. Therefore, a wedge and a trisector can merge and disappear: this is a *pairwise annihilation*. The reverse evolution is called a *pairwise creation*. Both are the equivalent of the fold bifurcations for critical points. An example is proposed in Fig. 17.8

17.3.3.2 Homogeneous mergings

When two linear degenerate points of the same nature merge, their half-integer indices are added and the resulting singularity exhibits a pattern corresponding to a linear critical point, e.g., two trisectors lead to a saddle point. However, according to what precedes, these new degenerate points are nonlinear and thus unstable. Details on that topic can be found in Delmarcelle [5].

17.3.3.3 Wedge bifurcation

Both existing types of wedges have the same index, $\frac{1}{2}$. As a consequence, the transition from

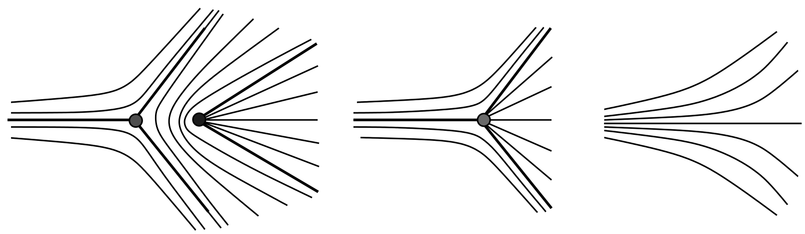

Figure 17.8 Pairwise annihilation of degenerate points.

one type to the other can take place without modifying structural consistency of the sur-
Q9 rounding flow. From a topological viewpoint, this evolution corresponds to the creation (resp. disappearance) of a parabolic sector along with an additional separatrix.

17.3.3.4 Global bifurcations

To finish this presentation of structural transitions in line fields, we briefly consider the simplest type of global bifurcation. It is intimately related to the unstable separatrices defined above. It occurs when the relative positions of two separatrices are changed through a common separatrix.

17.4 Topological Visualization of Vector and Tensor Fields

The theoretical framework described previously has motivated the design of techniques that build the visualization of vector and tensor fields upon the extraction and analysis of their topology. We start with a recall of the original method of Helman and Hesselink [9,10] for vector fields, later extended by Delmarcelle [5] to symmetric second-order tensor fields. After that, we focus on recent advances in topology-based visualization. New methods designed to complete the visualization of planar steady fields are discussed first. Nonlinear topology is addressed next. Techniques for reducing topological complexity in turbulent fields are considered, and the presentation ends with the topological visualization of parameter-dependent (e.g., unsteady) datasets. Throughout the presentation, we privilege a simultaneous treatment of vector and tensor techniques, making natural use of the profound theoretical relationships between their topologies.

17.4.1 Topology Basics

17.4.1.1 Original methods

Helman and Hesselink pioneered topology-based visualization in 1989 [9]. They proposed a scheme for 2D vector fields, restricting the characterization of critical points to a linear precision. Remember that this leads to a graph where saddles, spirals, and nodes are the vertices Q10
and separatrices at the edges, integrated along the eigendirections of the saddle points. They extended their technique to tangential vector fields defined over surfaces embedded in 3D space [10]. Streamsurfaces [13,22] are started along the separatrices. This was shown to permit the visualization of separation and attachment lines in some cases. At the same time, Globus et al. [8] suggested a similar technique to visualize the topology of 3D vector fields defined over curvilinear grids. They do not provide the separating surfaces associated with 3D saddles, but use glyphs to depict their structure locally and draw streamlines from them. Observe that all these methods require the integration of streamlines, which is typically carried out with a numerical scheme, e.g., Runge-Kutta with adaptive stepsize [21]. Analytical methods exist for piecewise linear vector fields over triangula- Q11
tions, resp. tetrehedrizations [18].

The topological approach for vector fields inspired Delmarcelle, who extended the original scheme to symmetric, second-order planar tensor fields [6] within his work on general techniques for tensor-field visualization [5]. Here, too, analysis is restricted to linear precision. The missing quantitative information carried by eigenvalues is inserted into the representation by means of color coding. Existing attempts to generalize this method to 3D tensor fields suffer from the inherent difficulty of locating 3D degenerate points [11,16]. Typically they lead to complicated polynomial systems of high degree and lack surfaces to partition the domain conveniently.

17.4.1.2 Closed orbits

The original topological method neglects the importance of closed orbits. As mentioned previously, these features play a major role in the flow structure, acting like sinks or sources and playing the role of additional separatrices. Moreover, they represent a challenging issue for numerical integration schemes used in practice, since every streamline that converges toward a closed orbit will result in an endless computation. A traditional but inaccurate way to solve this problem is to limit the number of integration steps. However, this does not permit us to distinguish a closed orbit from a slowly converging spiral, i.e., a spiral with high vorticity. Furthermore, this might be very inefficient if the number of iterations is set to a fairly large value to avoid a premature integration break. To overcome this deficiency, Wischgoll and Scheuermann [34] first proposed a method that properly identifies and locates closed orbits. Their basic idea is to detect on a cell-wise basis a periodic behavior during streamline integration. Practically, once a cell cycle has been inferred, a control is carried out over the edges of the concerned cells. This ensures that a streamline entering the cycle will remain trapped. If this condition is met and no critical point is present in the cycle, the Poincaré-Bendixon theorem [7] ensures that a closed orbit is contained in it. Precise location is obtained by looking for a fixed point of the Poincaré map [2]. The method was generalized to 3D by Wischgoll and Scheuermann [35]. Note that the extension to tensor fields is straightforward even if closed tensor lines are rare in practice.

17.4.1.3 Local topology

The definition of topology given previously does not specifically address vector fields defined over a bounded domain. As a matter of fact, the idea behind topology visualization is to partition the domain into subregions where all streamlines exhibit the same asymptotic behaviour. If the considered domain is infinite, this is equivalent to looking for subregions where all streamlines reach the same critical point both backward and forward. Now, scientific visualization is typically concerned with domains spanned by bounded grids. In this case, the boundary must be incorporated into the topology analysis: outflow parts behave as sinks, inflow parts as sources, and the points separating them as half-saddles. Scheuermann et al. proposed a method that identifies these regions along the boundaries of planar vector fields [23]. It assumes that the restriction of the vector field to the boundary is piecewise linear. Half saddles are located and separatrices are started there, forward and backward, to complete the local topology visualization. Observe that the same principle can be applied in 3D: half saddles are no longer points but closed curves from which stream surfaces can be drawn.

17.4.2 Nonlinear Topology

The methods introduced so far are limited to linear precision in the characterization of singular points. We saw previously that nonlinear critical or degenerate points are unstable. However, when imposed constraints exist (e.g., symmetry or incompressibility of the flow), they can be encountered. To extend existing methods, Scheuermann et al. [25] proposed a scheme for the extraction and visualization of higher-order critical points in 2D vector fields. The basic idea is to identify regions where the index is larger than 1 (or less than -1). In such regions, the original piecewise linear interpolant is replaced by a polynomial approximating function. The polynomial is designed in Clifford algebra, based on theoretical results presented by Scheuermann et al [24]. This permits us to infer the underlying presence of a critical point with arbitrary complexity, which is next modeled and visualized as shown in Fig. 17.9.

An alternative way to replace several close linear singularities by a higher-order one is suggested by Tricoche et al. [29]. It works with local grid deformations and can be applied to both tensor and planar vector fields. Moreover, it ensures continuity over the whole domain. Based on a mathematical background analoguous to that of Scheuermann et al. [25], Mann and Rockwood presented a scheme for the detection of arbitrary critical points in three dimensions [17]. Geometric algebra is used to compute the 3D index of a vector field, which is obtained as an integral over the surface of a cube. Getting back to the original ideas of Poincaré in his study of dynamical systems, Trotts et al. [26] proposed a method to extract and visualize the nonlinear structure of a "critical point at infinity" when the considered vector field is defined over an unbounded domain.

17.4.3 Topology Simplification

Topology-based visualization usually results in clear and synthetic depictions that ease analysis and interpretation. Yet turbulent flows, like those encountered in CFD simulations, lead to topologies exhibiting many structures of very small scale. Their proximity and interconnection in the global picture cause visual clutter with classical methods. This drawback is worsened by low-order interpolation schemes, typical in practice, that confuse the results by introducing artifacts. Therefore, there is a need for post-processing methods that permit clarification of the topologies by emphasizing the most meaningful properties of the flow and suppressing local details and numerical noise. The problem was first addressed by de Leeuw et al. [15] for vector planar fields. Pairs of interconnected critical points are pruned along with the corresponding edges while preserving consistency. The importance of sinks and sources is evaluated with respect to the surface of their

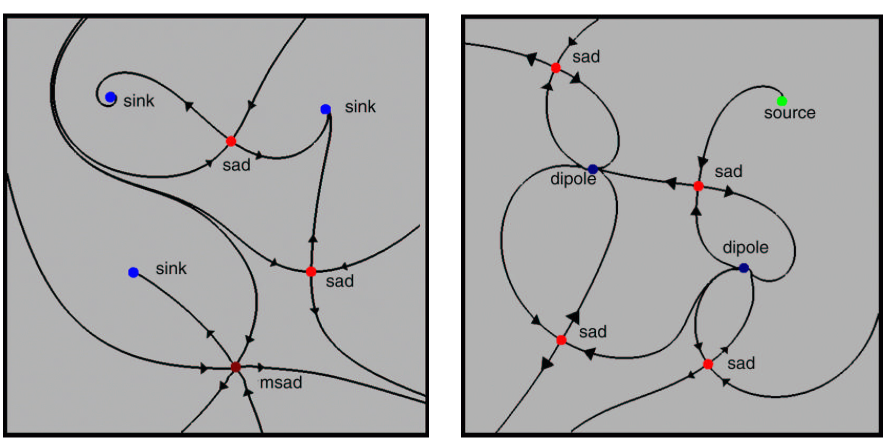

Figure 17.9 Nonlinear topologies

Q12

inflow (resp. outflow) regions. Since the method is graph-based, the resulting simplified topology lacks a corresponding vector-field description. Tricoche et al. [29] proposed an alternative approach for both vector and tensor fields defined in the plane. Close singularities are merged, resulting in a higher-order singularity that synthesizes the structural impact of small-scale features in the large scale. This reduces the number of singular points as well as the global complexity of the graph. The merging effect is achieved by local grid deformations that modify the vector field. There is no assumption about grid structure or interpolation scheme. The same authors presented a second method that works directly on the discrete values defined at the vertices of a triangulation [31]. Angle constraints drive a local modification of the vector field that removes pairs of singularities of opposite indices. This simulates a fold bifurcation. Results are shown in Fig. 17.10 for a vortex breakdown simulation. A major advantage compared to the previous method is that the simplification process can be controlled not only by geometric considerations but by arbitrary user-prescribed criteria (qualitative or quantitative, local or region-based), specific to the considered application.

17.4.4 Topology Tracking

Theoretical results show that bifurcations are the key to understanding and thus properly visualizing parameter-dependent flow fields: they transform the topology and explain how the stable structures arise that are observed for discrete values of the parameter. Typical examples in practice are time-dependent datasets. This basic observation motivates the design of techniques that permit us to accurately visualize the continuous evolution of topology. A first attempt was the method proposed by Helman and Hesselink [10]. The 1D parameter space is displayed in the third dimension (2D vector fields). However, the method is restricted to a graphical connection between the successive positions of critical points and associated sepatrices, leading to a ribbon if consistency was preserved. Thus, no connection is made if a structural transition has occurred: bifurcations are missed. The same restriction holds for the transposition of this technique to tensor fields by Delmarcelle and Hesselink [6]. Tricoche et al. [32,30] attacked this deficiency. The central idea of their technique is to handle the mathematical space, made of the euclidean space on one hand and the parameter space on the other hand, as a continuum. The vector or tensor

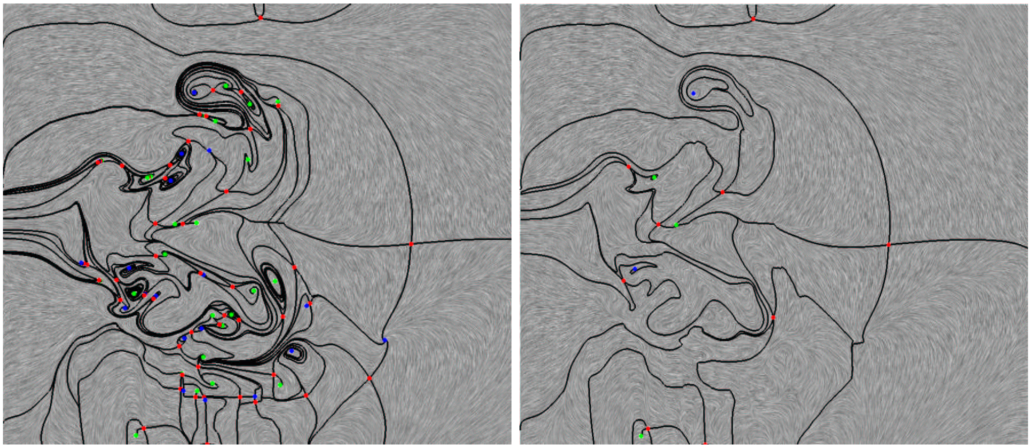

Figure 17.10 Turbulent and simplified topologies.

data are supposed to lie on a triangulation that remains constant. A "space–time" grid is constructed by linking corresponding triangles through prisms over the parameter space. The choice of a suitable interpolation scheme permits an accurate and efficient tracking of singular points through the grid along with the detection of local bifurcations on the way. With the scheme of [34], closed orbits are tracked in a similar way. Again, the technique results in a 3D representation. The paths followed by critical points are depicted as curves. Separatrices integrated from saddles and closed orbits span smooth separating surfaces. These surfaces are further used to detect modifications in the global topological connectivity: consistency breaks correspond to global bifurcations. Examples are proposed in Fig. 17.11.

17.5 Future Research

So far, the major limitation of many existing topological methods is their restriction to 2D datasets. This is especially true in the case of tensor fields. In fact, the basic idea behind topology, i.e., the structural partition of a flow into regions of homogenous behaviour, is definitely not restricted to two dimensions. However, the theoretical framework requires further research effort to serve as a basis for 3D visualization techniques. Now, in the simple case of linear precision in the characterization of critical points, topology-based visualization of 3D vector fields still lacks a fast, accurate, and robust technique to compute separating surfaces. This becomes challenging in regions of strong vorticity or in the vicinity of critical points, in particular for tur-bulent flows. In addition, topology-based visualization of parameter-dependent, 3D fields must overcome the limitations human beings experience in apprehending the information contained in 4D datasets.

Dealing with time-dependent vector fields, there is a fundamental issue with topology. The technique described in Section 17.4.4 addresses the visualization of the unsteady streamlines' topology. Remember that streamlines are defined as integral curves in steady vector fields. In the context of time-dependent vector fields, they must be thought of as instantaneous integral curves, i.e., the paths of particles that circulate with infinite speed. This might sound like a weird idea. Actually, this is a typical way for fluid dynamicists to investigate the structure of time-dependent vector fields in practice. Observe that there is no restriction to this tech-

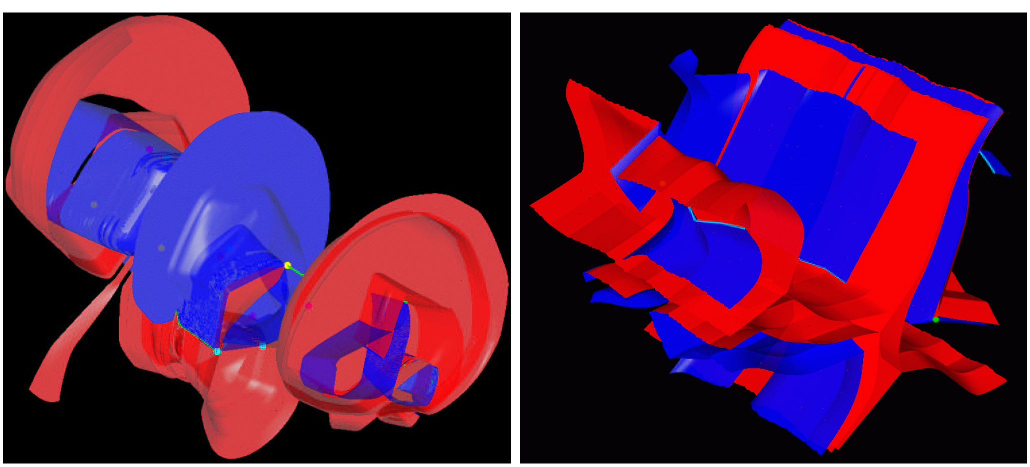

Figure 17.11 Unsteady vector and tensor topologies

nique for the visualization of parameter-dependent vector fields, this parameter not being time. Nevertheless, if one is interested in the structure of pathlines, i.e., the paths of particles that flow under the influence of a vector field varying over time, one has to rethink the notion of topology. As a matter of fact, the asymptotic behaviour of pathlines is not relevant for analysis, since there is no longer infinite time for them to converge toward critical points. Thus, a new approach is required to define ''interesting'' behaviors. Furthermore, a structural equivalence relation must be determined between pathlines, upon which a corresponding topology can be built. This seems to be a promising research direction, from both a theoretical and a practical viewpoint, to extend the scope of topological methods in the future.

References

1. A. A. Andronov, E. A. Leontovich, I. I. Gordon, and A. G. Maier. Qualitative theory of second-order dynamic systems. *Israel Program for Scientific Translations*, Jerusalem, 1973.
2. R. H. Abraham and C. D. Shaw. Dynamics: the geometry of behaviour I-IV. Aerial Press, Santa Cruz (Ca), 1982, 1983, 1985, 1988.
3. M. S. Chong, A. E. Perry and B. J. Cantwell. A general classification of three-dimensional flow fields. *Physics of Fluids*, A2(5):765–777, 1990.
4. U. Dallmann. Topological structures of three-dimensional flow separations. DFVLR-AVA Bericht Nr. 221–82 A 07, *Deutsche Forschungs- und Versuchsanstalt für Luft-und Raumgfahrt e. V.*, 1983.
5. T. Delmarcelle. *The visualization of second-order tensor fields*. PhD Thesis, Stanford University, 1994.
6. T. Delmarcelle and L. Hesselink. The topology of symmetric, second-order tensor fields. *IEEE Visualization '94 Proceedings*, IEEE Computer Society Press, Los Alamitos, pages 140–147, 1994.
7. J. Guckenheimer and P. Holmes. Nonlinear oszillations, dynamical systems and linear algebra. Springer, New York, 1983.
8. A. Globus, C. Levit and T. Lasinski. *A tool for the topology of three-dimensional vector fields*. *IEEE Visualization '91 Proceedings*, IEEE Computer Society Press, Los Alamitos, pages 33–40, 1991.
9. J. L. Helman and L. Hesselink. Representation and display of vector field topology in fluid flow data sets. *Computer*, 22(8):27–36, 1989.
10. J. L. Helman and L. Hesselink. Visualizing vector field topology in fluid flows. *IEEE Computer Graphics and Applications*, 11(3):36–46, 1991.
11. L. Hesselink, Y. Levy and Y. Lavin. The topology of symmetric, second-order 3D tensor fields. *IEEE Transactions on Visualization and Computer Graphics*, 3(1):1–11, 1997.
12. M. W. Hirsch and S. Smale. Differential equations, dynamical systems and linear algebra. Academic Press, New York, 1974.
13. J. P. M. Hultquist. Constructing stream surfaces in steady 3D vector fields. *IEEE Visualization '92 Proceedings*, IEEE Computer Society Press, Los Alamitos, pages 171–178, 1992.
14. M. J. Lighthill. Attachment and separation in three dimensional flow. *L. Rosenhead, Laminar Boundary Layers II*, Oxford University Press, Oxford, pages 72–82, 1963.
15. W. C. de Leeuw and R. van Liere. Collapsing flow topology using area metrics. *IEEE Visualization '99 Proceedings*, IEEE Computer Society Press, Los Alamitos, pages 349–354, 1999.
16. Y. Lavin, Y. Levy and L. Hesselink. Singularities in nonuniform tensor fields. *IEEE Visualization '97 Proceedings*, IEEE Computer Society Press, Los Alamitos, pages 59–66, 1997.
17. S. Mann and A. Rockwood. Computing singularities of 3D vector fields with geometric algebra. *IEEE Visualization '02*, IEEE Computer Society Press, Los Alamitos, pages 283–289, 2002.
18. G. M. Nielson and I.-H. Jung. Tools for computing tangent curves for linearly varying vector fields over tetrahedral domains. *IEEE Transactions on Visualization and Computer Graphics*, 5(4):360–372, 1999.
19. A. E. Perry and M. S. Chong. A description of eddying motions and flow patterns using critical point concepts. *Ann. Rev. Fluid Mech.*, pages 127–155, 1987.
20. H. Poincaré. Sur les courbes définies par une équation différentielle. *J. Math. 1*, pages 167–244, 1875. *J. Math. 2*, pages 151–217, 1876. *J. Math. 7*, pages 375–422, 1881. *J. Math. 8*, pages 251–296, 1882.
21. W. H. Press, S. A. Teukolsky, W. T. Vetterling and B. P. Flannery. *Numerical Recipes in C.* (2nd ed.) Cambridge, Cambridge University Press, 1992.
22. G. Scheuermann, T. Bobach, H. Hagen, K. Mahrous, B. Hahmann, K. I. Joy and W. Kollmann. A tetrahedra-based stream surface algorithm. *IEEE Visualization '01 Proceedings*, IEEE Computer Society Press, Los Alamitos, 2001.

23. G. Scheuermann, B. Hamann, K. I. Joy and W. Kollmann. Visualizing local topology. *Journal of Electronic Imaging* 9(4), 2000.
24. G. Scheuermann, H. Hagen and H. Krüger. An interesting class of polynomial vector fields. In Morton Daehlen, Tom Lyche, Larry L. Schumaker (eds.), *Mathematical Methods for Curves and Surfaces II*, Vanderbilt University Press, Nashville, pages 429–436, 1998.
25. G. Scheuermann, H. Krüger, M. Menzel and A. P. Rockwood. Visualizing nonlinear vector field topology. *IEEE Transactions on Visualization and Computer Graphics*, 4(2):109–116, 1998.
26. I. Trotts, D. Kenwright and R. Haimes. Critical points at infinity: a missing link in vector field topology. *NSF/DoE Lake Tahoe Workshop on Hierarchical Approximation and Geometrical Methods for Scientific Visualization*, 2000.
27. M. Tobak and D. J. Peake. Topology of three-dimensional separated flows. *Ann. Rev. Fluid Mechanics*, 14:81–85, 1982.
28. X. Tricoche. Vector and tensor topology simplification, tracking, and visualization. *Ph.D. thesis, Schriftenreihe FB Informatik 3*, University of Kaiserslautern, Germany, 2002.
29. X. Tricoche, G. Scheuermann and H. Hagen. Vector and tensor field topology simplification on irregular grids. *Data Visualization 2001 - Proceedings of the Joint Eurographics - IEEE TCVG Symposium on Visualization*, Springer, Wien, pages 107–116, 2001.
30. X. Tricoche, G. Scheuermann and H. Hagen. Tensor topology tracking: a visualization method for time-dependent 2D symmetric tensor fields. *Eurographics '01 Proceedings*, Computer Graphics Forum 20(3):461–470, 2001.
31. X. Tricoche, G. Scheuermann and H. Hagen. Continuous topology simplification of 2D vector fields. *IEEE Visualization '01 Proceedings*, IEEE Computer Society Press, Los Alamitos, 2001.
32. X. Tricoche, T. Wischgoll, G. Scheuermann and H. Hagen. Topology tracking for the visualization of time-dependent two-dimensional flows. *Computers & Graphics 26*, pages 249–257, 2002.
33. R. Westermann, C. Johnson and T. Ertl. Topology-preserving smoothing of vector fields. *IEEE Transactions on Visualization and Computer Graphics*, 7(3), pages 222–229, 2001.
34. T. Wischgoll and G. Scheuermann. Detection and visualization of closed streamlines in planar flows. *IEEE Transactions on Visualization and Computer Graphics*, 7(2):165–172, 2001.
35. T. Wischgoll and G. Scheuermann. 3D loop detection and visualization in vector fields. *To appear in "Mathematical Visualization" (Vismath 2002 Proceedings)*, 2003.

AUTHOR QUERIES

Q1 Au: ok?
Q2 Au: please spell out?
Q3 Au: ok?
Q4 Au: please spell out?
Q5 Au: ok?
Q6 Au: ok?
Q7 Au: please clarify?
Q8 Au: another what?
Q9 Au: please spell out?
Q10 Au: ok?
Q11 Au: please spell out?
Q12 Au: